Influence of Fines Dissolving on Crystal Size Distribution in an MSMPR Crystallizer

PAWEL JUZASZEK
and
M. A. LARSON

Department of Chemical Engineering and The Engineering Research Institute
Iowa State University
Ames, Iowa

A laboratory mixed suspension mixed product removal (MSMPR) crystallizer was operated with and without continuous fines segregation and destruction. Predicted improvements in product-crystal size were observed. By carefully representing the crystallizer flow pattern, quantitative agreement of crystal size distribution with prediction was achieved.

SCOPE

The quantitative evaluation of fines dissolving techniques for increasing crystal size in crystallizers is necessary for proper design of such systems. Previous theoretical analyses have predicted the effect of such techniques, but industrial systems have only shown a qualitative response to the imposition of fines dissolving. The present work involved the operation of a laboratory mixed-suspension mixed product removal (MSMPR) crystallizer with and without fines segregation and destruction. The effects of different flow patterns in the fines trap were examined, and the crystallization kinetic parameters for potassium nitrate were determined under both conditions. The purpose of this work was to determine, under carefully controlled conditions, if CSD could be accurately predicted under fines segregation and dissolving conditions.

CONCLUSIONS AND SIGNIFICANCE

The crystal size distributions predicted by analysis using the population balance accurately reflect the actual size distribution obtained in an MSMPR crystallizer if the flow pattern in the system is well known. The size distribution of the small crystal portion of the size range can be accurately predicted with a knowledge of the midrange distribution, the recirculation flow rates, and the settling velocities of crystals. Experimental growth kinetics were unchanged under conditions of fines dissolving, but experimental nucleation kinetics obtained under conditions of fines dissolving were of higher order than without fines dissolving. This suggests that secondary nucleation is not well understood, and apparently observed kinetics are intimately related to nuclei survival.

Laminar flow in a fines trap, such as that used in the draft tube baffle (DTB) crystallizer, will have a distinct effect on the trap's ability to achieve a distinct crystal size cut at a predetermined size. Moreover, nonideal flow patterns in the crystallizer body itself can lead to classified product removal as well as nonideal fines removal.

Careful analysis of flow patterns in industrial crystallizers, along with a good knowledge of settling velocities of the crystalline material, can lead to improved design of fines destruction units in continuous crystallization.

One of the most common methods for controlling crystal size distribution in continuous crystallizers is by continuous destruction of fines. The first published theoretical analysis of the effect of fines dissolving on crystal size distribution (CSD) was presented by Saeman (1956). This analysis was later extended by Randolph and Larson (1971). The basic analysis technique of these authors was the use of the crystal population balance to develop a model for the CSD relating CSD to process configuration and crystallization kinetics.

In modeling the fines dissolving influence on CSD in an MSMPR crystallizer, they assumed an ideal fines trap through which part of the suspension is removed from the crystallizer as shown in Figure 1. The upward flow in this fines trap is such that all crystals exceeding a cut size L_F are held and returned to the crystallizer body, permitting only crystals less than size L_F to be removed. The fines suspension removed can be used for subsequent treatment, or the fines can be dissolved by heating and the liquor returned to the crystallizer. The imposition of fines dissolving and subsequent liquor return, while at the same time maintaining a given net crystal production rate, causes an increase in supersaturation. This results in higher nucleation and growth rates and reduces, to some degree, the desired effect of fines dissolving.

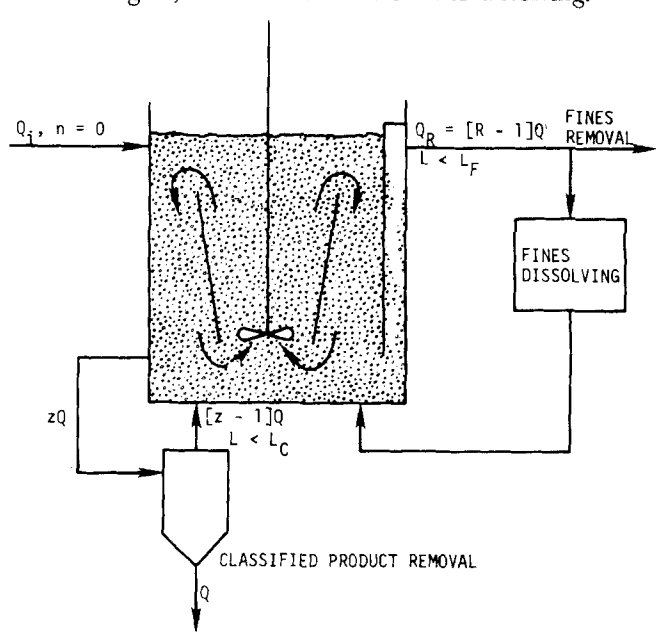

Fig. 1. Fines destruction crystallizer.

Correspondence concerning this paper should be addressed to M. A. Larson. Pawel Juzaszek is at the Institute of Chemical Engineering, Polytechnical University of Warsaw, Warsaw, Poland.

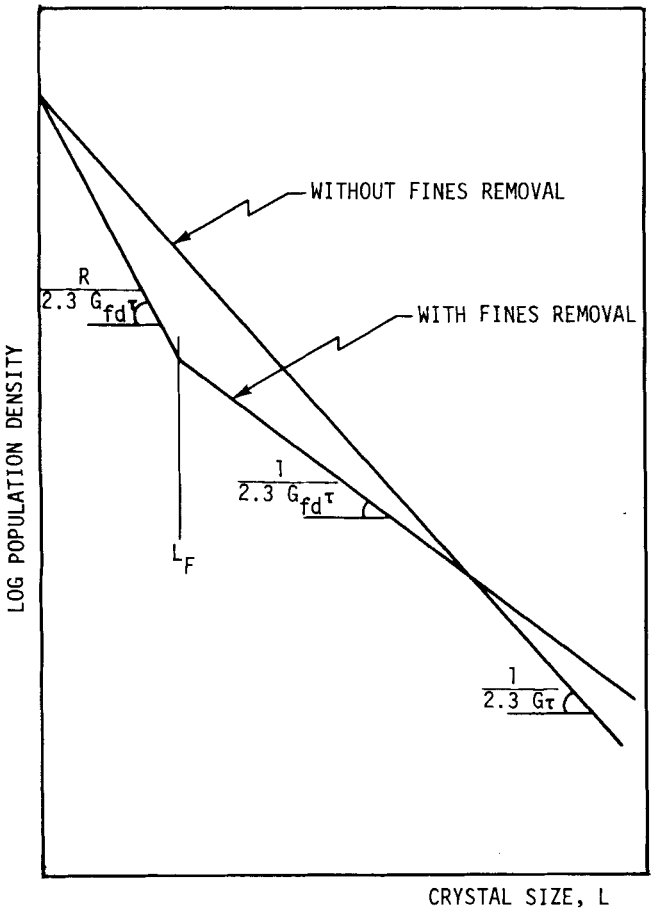

Fig. 2. Effect of fines destruction on CSD.

A number balance over the above described system, assuming McCabe's ΔL law appplies, gives the following expression for the population density distribution:

$$n = n^o \exp\left[-\frac{RL}{G\tau}\right] \qquad L < L_F$$

$$n = n^o \exp\left[-\frac{(R-1)L_F}{G\tau}\right] \exp\left[-\frac{L}{G\tau}\right] \qquad L > L_F \tag{1}$$

The comparison of the size distribution of crystallizers with and without fines destruction is shown in Figure 2.

The value of fines destruction has been demonstrated industrially in a qualitative way, especially by the draft tube baffle (DTB) design. Unfortunately, the distributions obtained, while improved, are not represented by Equation (1) and, it is, therefore, difficult to design these crystallizers through the direct use of theoretical equations. There is insufficient, carefully obtained, experimental data to confirm that Equation (1) does in fact represent an obtainable size distribution.

This paper describes an attempt to experimentally investigate the influence of fines dissolving on CSD and also gives an analysis using results from crystallization kinetics research for prediction of crystal size distributions in a crystallizer with fines destruction.

EXPERIMENTAL APPARATUS AND PROCEDURE

The research apparatus was a laboratory MSMPR crystallizer with a cooling system with an operating capacity of 10 l as described by Helt (in press). For the purpose of this investigation, the device was additionally equipped with a fines trap and fines destruction system. The modified process flow diagram is shown in Figure 3.

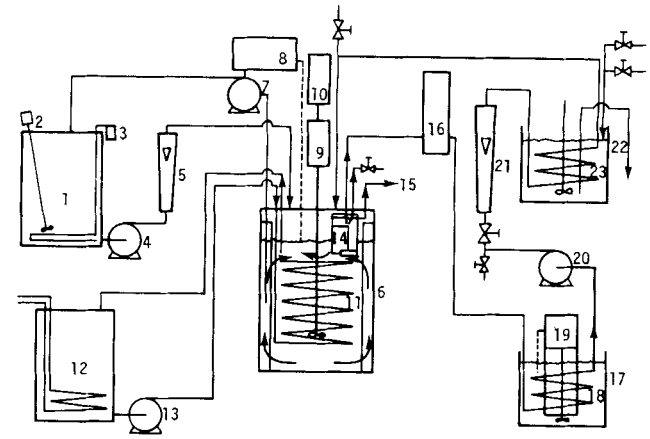

1. TEMPERATURE CONTROLLED TANK
2. STIRRER
3. FEED TANK HEATING CONTROL
4. FEED PUMP
5. FEED LINE ROTAMETER
6. CRYSTALLIZER VESSEL
7. WITHDRAWAL PUMP
8. LIQUID LEVEL REGULATION SYSTEM
9. STIRRER MOTOR
10. STIRRER VARIAC SYSTEM
11. CRYSTALLIZER COOLING COIL
12. COOLANT SUPPLY TANK
13. COOLANT PUMP
14. FINES TRAP
15. FINES SAMPLE WITHDRAWAL PORT
16. ELECTRIC HEATER
17. STAINLESS STEEL WATER HEATER
18. ELECTRIC HEATER
19. FINES DISSOLVING TEMPERATURE CONTROL SYSTEM
20. CIRCULATION PUMP
21. FINES REMOVAL LINE ROTAMETER
22. WATER COOLING DEVICE (HEAT EXCHANGER)
23. COOLING COIL

Fig. 3. Experimental apparatus.

MSMPR Crystallizer

With reference to Figure 3, an overheated aqueous solution of potassium nitrate prepared in the temperature controlled tank (1) was pumped to the crystallizer (6). The feed flow was measured with a rotameter (5). The crystal suspension was removed from the crystallizer with a pump (7), which was controlled by a liquid level regulation system (8), and was returned to the feed tank.

The crystallizer was a cylindrical vessel of Plexiglas with a propeller type of agitator, three baffles, and a stainless steel cooling coil that also served as a draft tube. The tube for isokinetic removal of suspension was placed between the draft tube and the crystallizer wall at a height approximately equal to half the level of suspension in the crystallizer.

Fines Dissolving System

The fines dissolving system consisted of the fines trap (14), an electric heater (16), a stainless steel water heater (17), a circulation pump (20), a rotameter (21), and a water cooling device (22). The liquor containing fines was passed through the trap, heated in heaters (16,18) until fines were dissolved, and then cooled in a heat exchanger (22) to a temperature 1/2°C greater than the crystallizer. It was then returned to the crystallizer. A detail of the fines trap is shown in Figure 4. The fines trap contained three compartments so that various upward suspension velocities could be obtained by merely moving the flexible part of the tube (2). The temperature in the fines dissolver was kept at more than 4°C higher than the crystallizer in order to assure that the nuclei and small crystals were destroyed. Because secondary nucleation is known to be the prime source of nuclei, no nucleation was experienced in the return cooler of the fines removal system. Secondary nucleation requires the presence of macrosized crystals. This was confirmed by Coulter counter analysis of the return stream.

Experiment

Crystallization of potassium nitrate was initially carried out without fines removal until steady state was reached. This usually required ten to twenty retention times. The crystal size distribution was determined. Fines removal and destruction were then imposed, and after steady state was reached, the size distribution of the fines and the product were determined. During the experiment the following quantities were measured: feed flow, fines dissolver flow, and temperatures of all vessels and streams.

To obtain size distributions, suspensions were taken from the crystallizer and the fines trap using a vacuum bottle. The

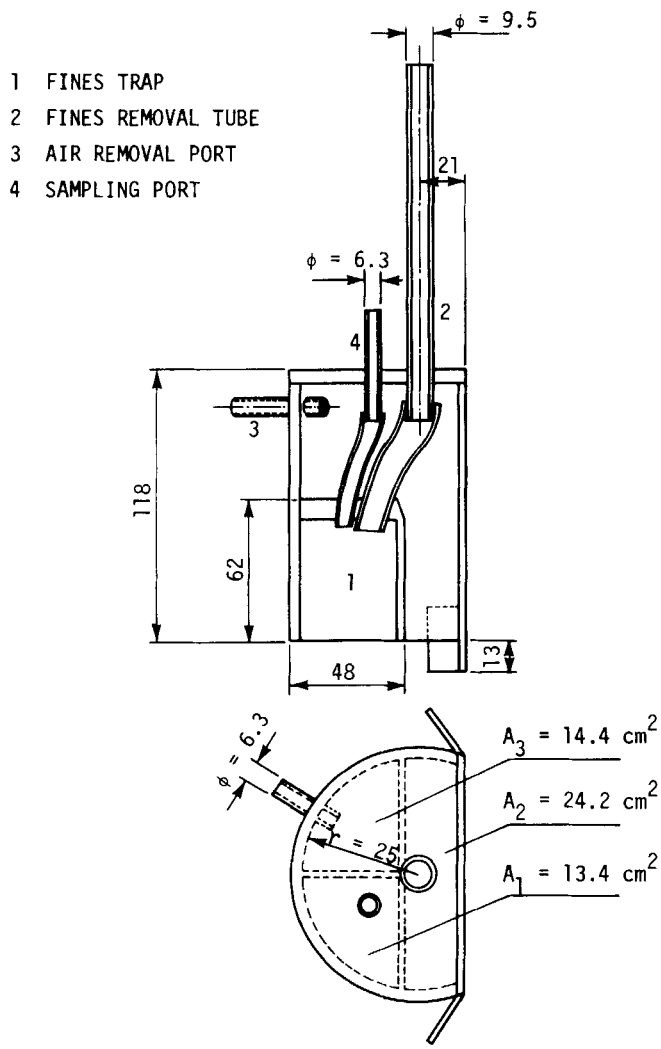

Fig. 4. Fines trap.

crystals were separated from the liquor with a buchner filter, washed with acetone, dried and sized using sieves.

EXPERIMENTAL RESULTS

In order to determine the fines dissolving influence on crystal size distribution, the experiments were carried out so that CSD could be determined with and without fines destruction, keeping all other operating conditions constant. While the sequence of runs with differing process conditions was optional, in all cases the nonfines dissolving data were taken immediately prior to the corresponding fines dissolving run. The variables that changed from one set of experiments to another were mean retention time and recirculation ratio R. The cut size L_F was changed by regulating the recirculation rate and the active flow area in the fines trap. The temperature in the crystallizer was not changed, but the fines dissolving temperature was changed for some experiments.

Typical CSD's, both with and without fines dissolving, are shown in Figures 5 through 9. The straight line semilog population density plots show that the data for the runs conducted in the absence of fines dissolving agree with the distribution function predicted by the analysis of Randolph and Larson (1971) for the case when McCabes Δ_L law holds. Only in the large sizes, sizes greater than 600 μm, is there a distinct deviation from a straight line. That this effect appears also in the fines dissolving experiments indicates the existence of internal classification in the crystallizer. This effect will be discussed in detail later. In the fines dissolving ex-

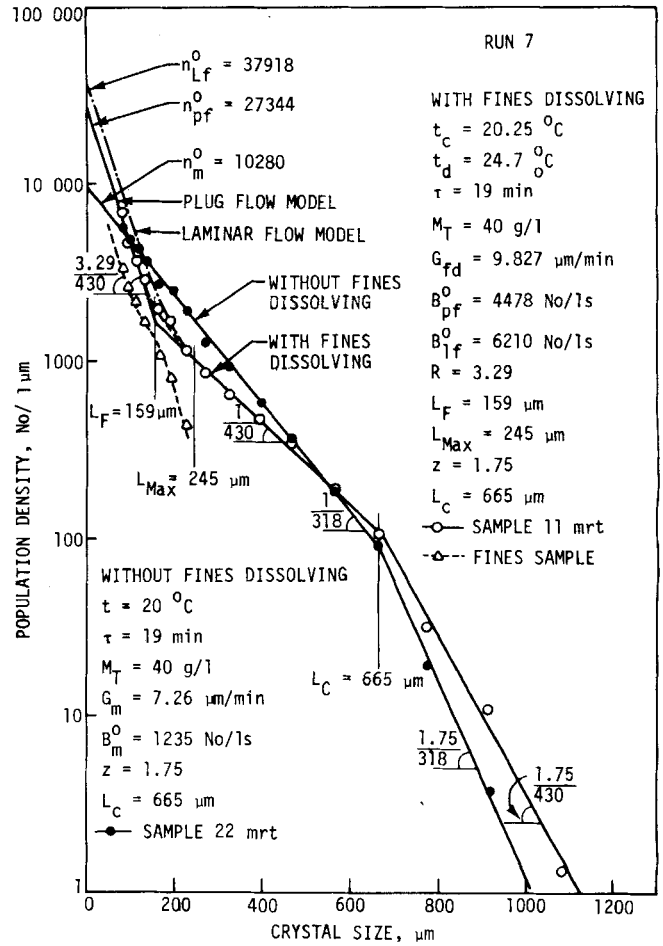

Fig. 5. CSD from run 7.

periments, the distribution deviates from a straight line in the small size range in accordance with the theoretical predictions of Randolph and Larson (1971). The deviation, however, is not a sharp intersection of two straight lines with a distinct cut size L_F. It is spread over a fairly wide range of sizes. Nevertheless, an evident relationship between CSD and trap operation parameters can be observed. In all experiments, this deviation appears in the area of the predicted cut size L_F. Comparison of the slopes of the product crystals with and without fines removal shows that the growth rate in the former case is greater. This is the expected result, because when fines are dissolved and net production rate is held constant supersaturation must be higher.

Cut Size L_F

The cut size L_F, the largest crystal withdrawn in the fines trap, was calculated assuming plug flow. The linear velocity of the suspension in the fines trap is therefore defined by

$$u_p = Q_R/A \qquad (2)$$

In an ideal system, only crystals that have a terminal settling velocity less than u_p will be carried out of the crystallizer through the trap. Thus, the cut size L_F is that size which has a terminal velocity u_p. The terminal settling velocities in the mother liquor of potassium nitrate crystals of various sizes were determined experimentally and are given in Table 1 along with the ratio of the size $\overline{L}$ to the equivalent spherical diameter. These data are plotted in Figure 10 along with the calculated spherical particles' terminal velocities. These latter velocities were determined using standard friction factor correlations. With a knowledge of the linear velocity

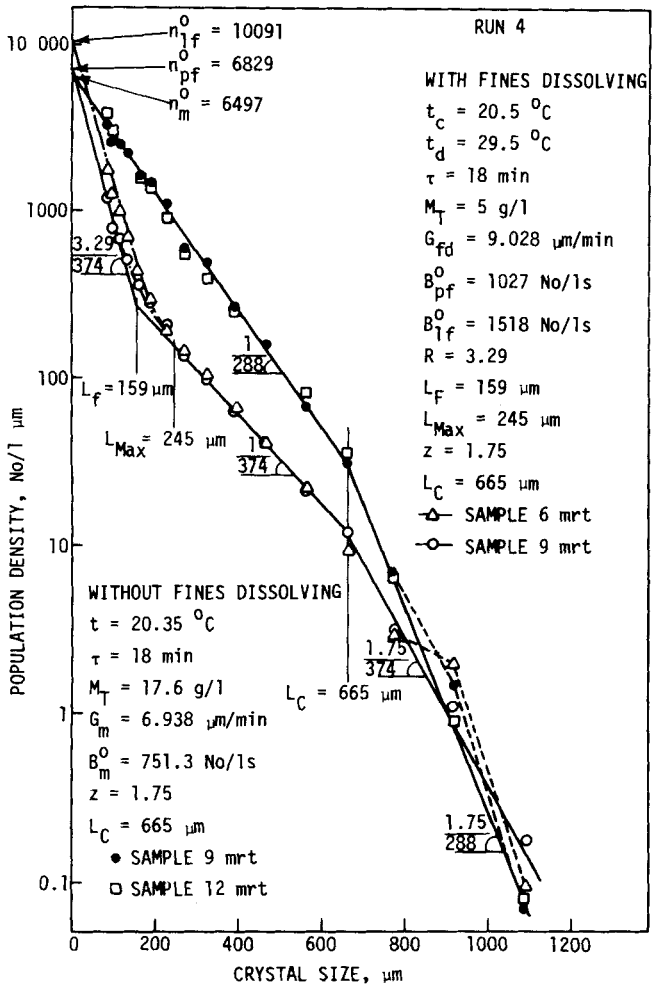

Fig. 6. CSD from run 4.

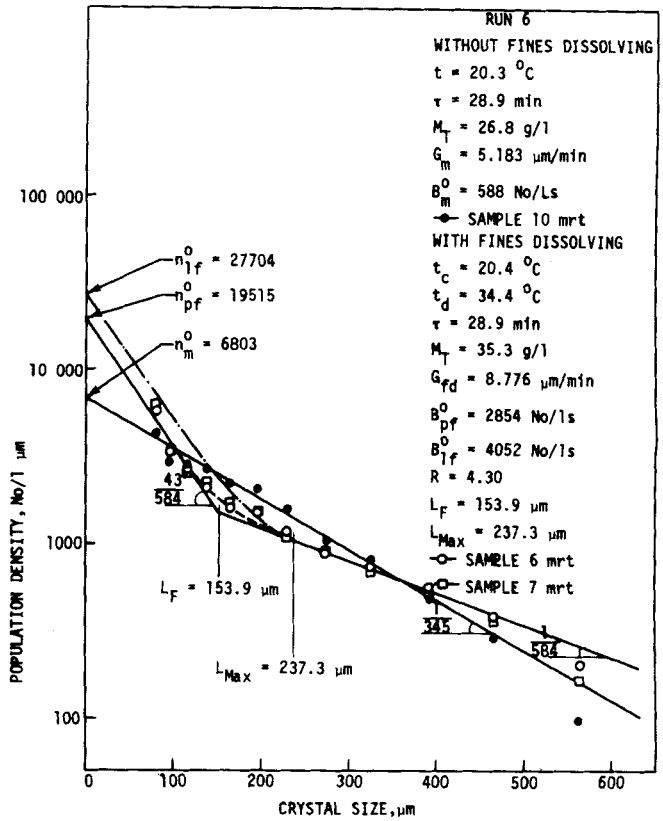

Fig. 7. CSD from run 6.

of liquid in the fines trap, the cut size L_F was determined from Figure 10 and used in Figures 5 to 9 to determine the intersection of the distribution of the fines and the product crystals. Growth rate was determined from the slope of the distribution of the large crystals, and the slope of the distribution of the fines was determined using this growth rate and a knowledge of the flow rate through the fines trap. Good agreement with the data was obtained. The curved portion of the experimental curve near the cut size L_F is expected because a precise cut is normally not possible owing to the velocity profile in the fines dissolver.

Internal Classification Influence on CSD

In all experiments with and without fines dissolving, the population density plots change slope rapidly near crystal size $L_c \approx 660$ μm. Beyond this point, the distribution becomes linear again with the slope about 1.7 times the slope of the central part of the distribution curve. This phenomenon reflects the conclusion of Randolph (1965) for classified product removal on CSD.

Table 1. Potassium Nitrate Terminal Settling Velocities in Mother Liqhor at 20.3°C

Crystal size, μm	$\bar{L}$, μm	$\bar{u}_s$, cm/s	$\bar{L}/d_s$
180-200	189.74	2.07	0.759
160-180	169.70	1.745	0.761
150-160	154.92	1.52	0.763
125-150	136.93	1.28	0.7565
112-125	118.32	0.995	0.763

The Randolph model (see Figure 1) assumes that the crystals in the product stream are sized such that all crystals greater than size L_c are permanently removed, but a representative fraction of crystals smaller than size L_c are returned to the crystallizer. The large crystals are removed Z times faster than the smaller crystals. An analogous situation is suggested by the distributions presented in Figures 5 and 6.

The curves in Figures 5 and 6 are represented by Equation (1) for sizes less than L_c and for sizes greater than L_c by

$$n = C_1 \exp\left(-\frac{ZL}{G\tau}\right) \quad L > L_c \tag{3}$$

The value C_1 is implied by the necessity for continuity:

$$C_1 = n^o \exp\left[\frac{(Z-1)L_c - (R-1)L_F}{G\tau}\right] \tag{4}$$

From the above analysis, it appears that crystals greater than about size 660 μm were removed 1.7 times faster than crystals smaller than 660 μm. Usual observations of the suspension movement in the region surrounding the suspension removal points confirmed the potential for this phenomenon to occur. The intensity of stirring was sufficient to keep crystals in suspension because no crystals collected on the bottom of the vessel; nevertheless, it was observed that an ideal slurry distribution was not obtained. In the space between the baffles, wall, and draft tube, where the suspension was moving upwards, dead zones occurred and had the form of stable circulation loops of concentrated slurry containing more large crystals than the flow stream. The main flow stream passed through the center of these zones with a relatively homogeneous suspension of crystals. Figure 11 illustrates the CSD in a sample taken from such a dead zone in an experiment without fines dissolving. As shown in the plot, the distribution is well approximated by a straight

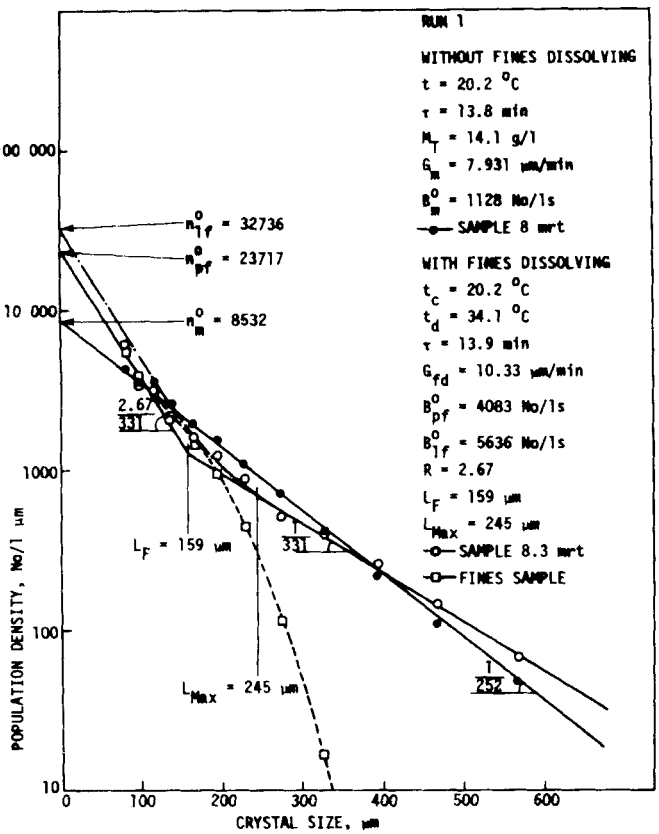

Fig. 8. CSD from run 1.

line up to around 600 μm; then the increase in large crystal population density becomes evident. Such a distribution corresponds to the solution of the total population balance for a product stream with classified product removal. The hypothetical shape of this crystallizer distribution resulting from this classified removal is shown by the dashed line in Figure 11. It was observed that, fortuitously, the crystallizer was constructed in such a way that the suspension removal point was located in the proximity of a dead zone but not in the zone. Hence, the removed suspension was enriched with large crystals but to a less extent than is implied by Figure 11.

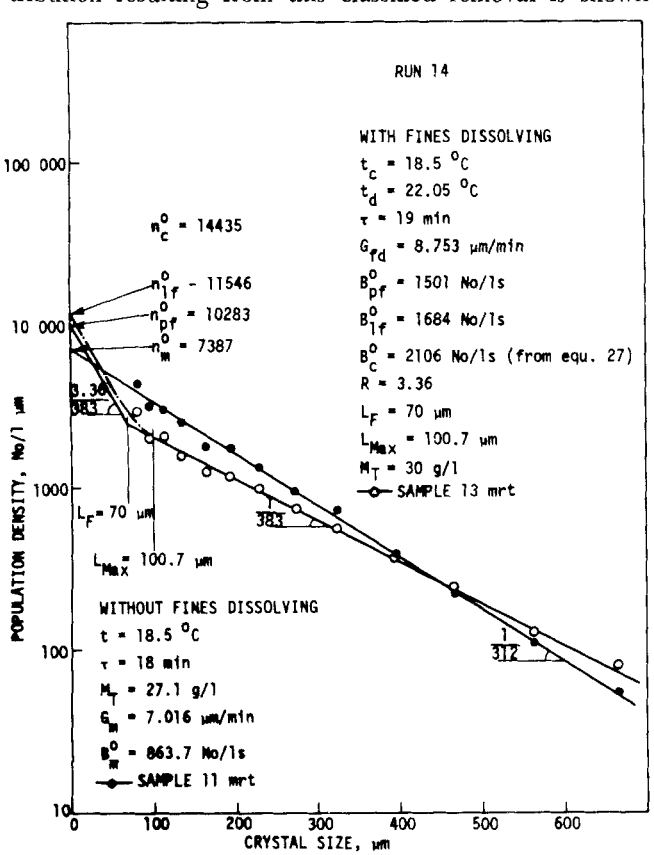

Fig. 9. CSD from run 14.

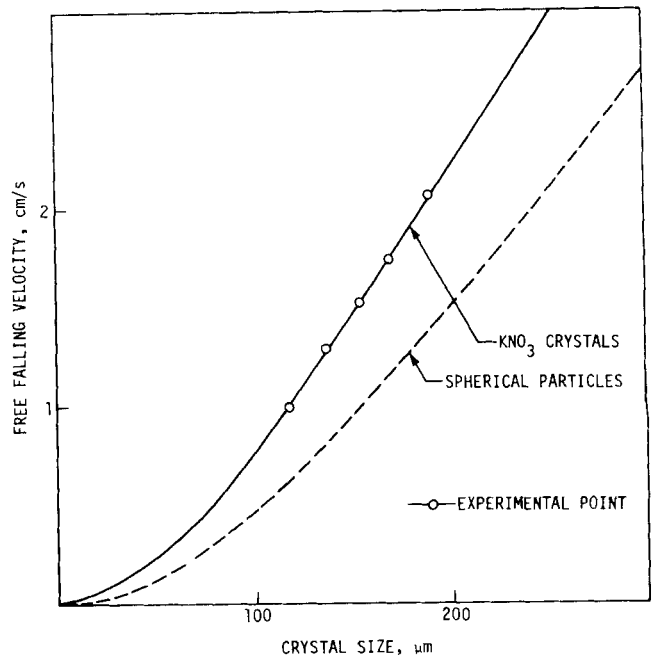

Fig. 10. Settling velocity of potassium nitrate crystals.

It is not the intent of this paper to go into details of the classified suspension removal problem; however, it is possible to address this problem in the context of the crystallizer design and explain the deviations from the MSMPR distribution observed. In all of the runs, the size L_c remained substantially the same because the withdrawal location was unchanged. In a Krystal Crystallizer or other type of crystallizer which exhibits nonisotropic flow, the size of crystals dominating the distribution changes with height. In these experiments, withdrawal was always at the same height.

After preliminary experiments in which the classified removal effect was noticed, sampling was done at various heights and positions. In these instances, different L_c's were obtained, but the results were always consistent for a given location.

From the observation described in the previous paragraphs, the following conclusions can be drawn:

1. Sampling in these experiments produced predicted size distributions for crystals smaller than L_c. Therefore, the crystallizer as a whole can be considered to be an ideal MSMPR crystallizer with classified product removal at size $L_c = 660$ μm.

2. The linear distribution in the range free from fines removal and classification effects indicates McCabe's Δ_L law holds. In addition, the crystal size range below 660 μm can be considered free from classification effects and the distribution dependent only on the nucleation and growth rates and fines removal effects. This assumption is fundamental to the evaluation of the results given in subsequent paragraphs.

MSMPR Kinetic Data

The kinetic relationships for nucleation and growth were determined from size distribution data taken from experiments which did not employ fines dissolving. The CSD results from a screen analysis of suspension samples taken in the final moments of an MSMPR run were

TABLE 2. MSMPR KINETIC DATA

Run number	Mean retention time τ, min	Process temperature t, °C	Suspension density M_T, g/l	Growth rate G, μm/min	Effective population density of nuclei n^o No/μml	Effective nucleation rate B^o, No/ls	$\frac{B^o}{M_T^{0.5}}$
1	13.8	20.2	14.1	7.93	8 530	1 130	300
2	17.3	20.2	12.7	6.67	6 710	750	209
3	18	20.3	15.8	7.43	5 530	690	172
4	18	20.4	17.6	6.94	6 500	750	179
7	19	20	40	7.26	10 280	1 240	195
8	19	20	33.6	6.81	11 100	1 260	217
9	19	19.8	21.6	6.74	6 800	760	164
10	19	20.3	19.2	6.48	7 430	800	182
11	19	20.3	18.4	6.72	6 300	710	164
6	28.9	20.3	26.8	5.18	6 800	590	113
12	29.3	20.3	10	4.61	3 170	240	17
17	19	18.5	14.5	6.23	6 030	630	164
16	19	18.5	17	6.55	5 830	640	154
15	18.6	18.1	20	7.09	5 926	700	156
14	19	18.5	27.1	7.02	7 390	864	165

analyzed to obtain the population density as a function of size. These data were plotted as shown in Figures 5 to 9. Data for sizes below 500 μm were used to evaluate the nucleation and growth rates with the aid of a computer. The parameters n^o and G were determined by a least-squares fit. These results are shown in Table 2. The results were then correlated using the equation

$$B^o = k_N G^i M_T^j \tag{5}$$

The data were best correlated using $j = 0.5$ and a least-squares technique to determine $k_n = 3.65$ and $i = 2.06$. The resulting plot of this kinetic relationship is shown in Figure 12, where the coordinates are $B^o/M_T^{0.5}$ and G, respectively. The slope of the line is 2.06.

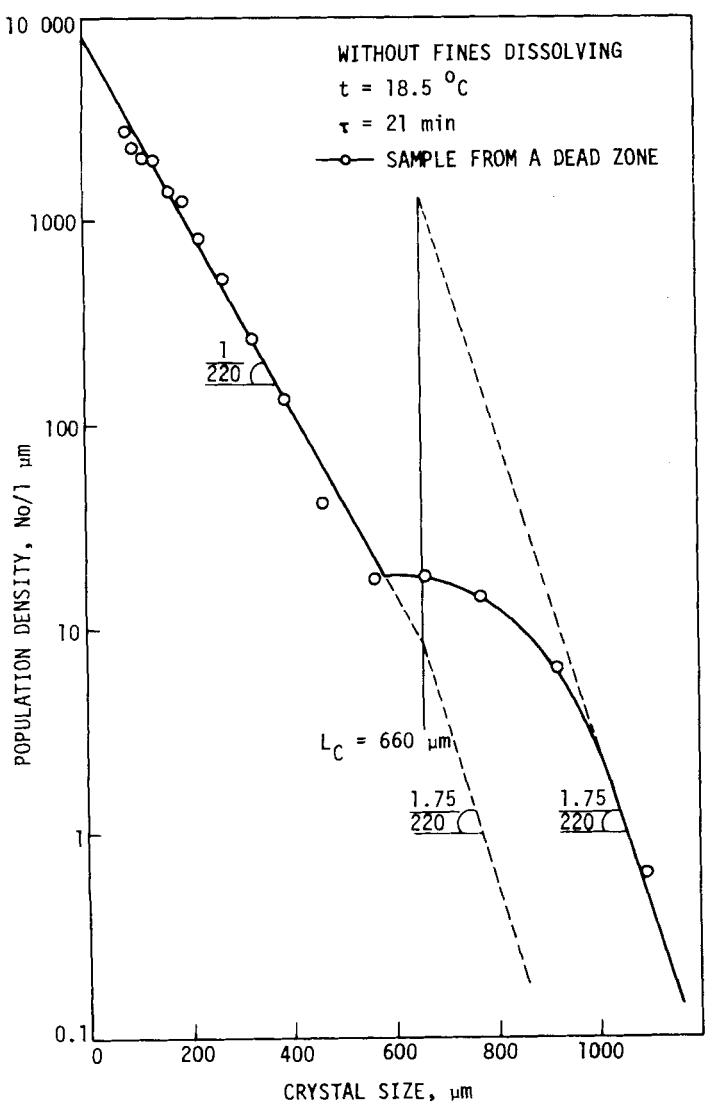

Fig. 11. Distribution of crystals in a dead zone.

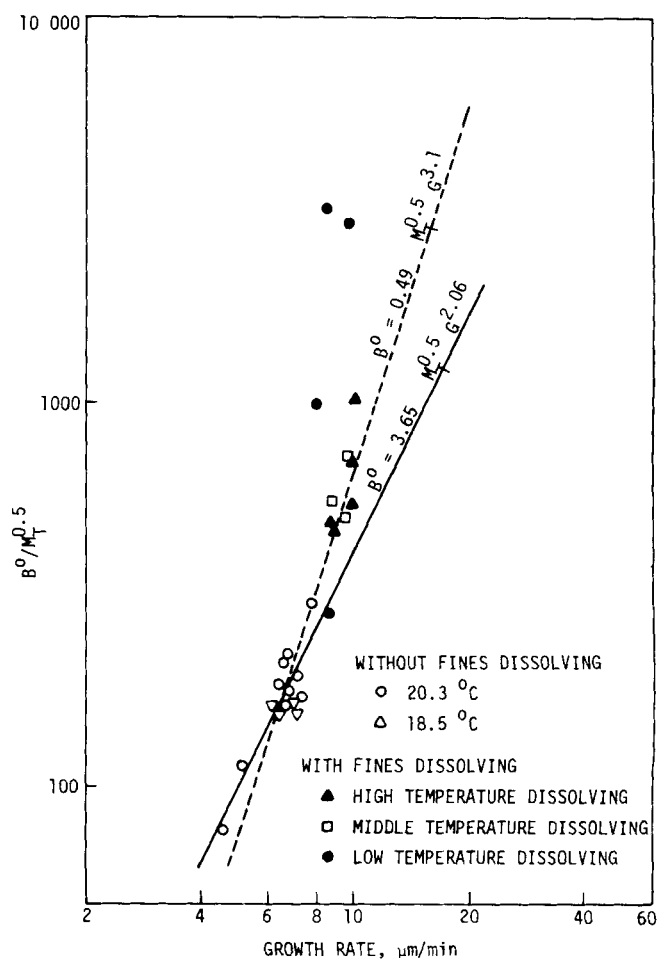

Fig. 12. Nucleation kinetics correlation.

Table 3. Fines Dissolving Kinetic Data

Mean retention time, min	Process temperature t_c, °C	Fines dissolving temp., °C	Circulation R	L_F, m	L_{max}, μm	Growth rate G, μm/min	Run number	Effective population density of nuclei: Plug flow model n^o_{pf} $No/1$ μm	Effective population density of nuclei: Laminar flow model n^o_{lf} $No/1$ μm	Effective nucleation rate: Plug flow model B^o_{pf}, $No/1s$	Effective nucleation rate: Laminar flow model B^o_{lf}, $No/1s$	Suspension density M_T, g/l	$\frac{B^o}{M_T^{0.5}}$
13.9	20.2	34.1	2.67	159	245	10.3	1	23 700	32 700	4 080	5 640	16.1	1 020
17.3	20.6	34.5	3.18	159	245	10.6	2	4 700	6 500	830	1 150	5.5	350
18	20.5	31.8	3.29	159	245	10.1	3	12 300	17 400	2 060	2 920	14.4	540
18	20.5	29.5	3.29	159	245	9.0	4	6 800	10 091	1 030	1 520	5	460
19	20.3	34.0	3.29	159	245	10.0	5	16 000	22 300	2 670	3 720	14.6	700
28.9	20.4	34.4	4.30	154	237	8.8	6	19 500	27 700	2 850	4 050	35.3	487
19	20.3	24.7	3.29	159	245	9.8	7	27 300	37 900	4 480	6 210	40	710
19	20.3	23.3	3.29	159	245	9.7	13	14 600	20 500	2 370	3 330	21.9	510
19	19.8	22.9	3.14	152	235	8.9	9	17 000	23 800	2 540	3 560	20.8	560
19	18.5	22.1	3.36	70	100	8.7	14	10 300	11 500	1 500	1 680	30	270
19	20.3	22.2	3.29	159	245	8.1	10	30 100	45 500	4 070	6 150	16.8	990
19	18.5	20.8	6.50	118	181	8.6	17	72 000	145 900	10 460	20 880	11	3 150
18.6	18.4	20.6	6.55	118	182	9.9	15	87 300	162 900	14 400	26 900	25	2 880

Kinetic Data with Fines Dissolving

Unlike the distributions discussed above, CSD's for processes with fines dissolving are distinguished by a region which deviates from a straight line on a semilog plot. This deviation is not a sharp change in slope predicted by theory but is a transition region around the cut size L_F. This region, shown as a dotted line in Figures 5 to 8, has no a priori boundary. It is assumed that all conclusions concerning the influence of fines liquor removal velocity, drawn from Randolph and Larson's model, remain valid, and, hence, the spreading of the transition region in the CSD is caused only by deviations from suspension plug flow in the fines trap.

Because of deviation from plug flow in the trap, not all crystals larger than L_F were held and returned to the crystallizer; some of these larger crystals, those carried in that portion of the stream with a velocity greater than average, were removed from the crystallizer through the trap. On the other hand, the existence of a portion of the liquor stream with a velocity lower than average caused a less than expected removal of small crystals. Such an explanation has validity because the Reynolds number for flow on the trap was of order 650. Clearly, the flow length of the trap was insufficient for the characteristic parabolic laminar velocity profile to form. However, this very low Reynolds number suggests that a certain degree of velocity deviation from plug flow did exist. In fully developed laminar flow in pipes, the maximum linear velocity is twice the mean flow velocity. Therefore, the maximum size of crystals carried, L_{max}, should have a settling velocity equal to twice the mean flow velocity. Values of L_{max} calculated for this condition are given in Table 3 and indicated on Figures 5 to 9. In all cases, the distribution deviation from theory does not exceed the calculated L_{max}. The effects of fines classification and product classification could be removed, therefore, by considering the range of sizes between L_c and L_{max}. From this size range, the growth rate G could be determined. Values obtained are given in Table 3. Two values for the nucleation rate were determined using Equation (1), assuming plug flow and laminar flow in the fines trap.

Nucleation Rate Assuming Plug Flow

To determine nucleation rate, values G, L_F and R were assigned and substituted into Equation (1). Growth rate G was determined from the slope of the middle portion of the distribution; L_F was calculated from flow velocities as previously described, and R, the fines liquor recirculation rates, was calculated by

$$R = \frac{Q_R + Q}{Q} \tag{6}$$

The value of $n_{(L_F)}$, the ordinate of the middle straight line portion of the distribution at L_F, was obtained from the plot of the data. The nuclei population density n_{pf}^o was found by transforming the first part of Equation (1) and evaluating at $L = L_F$:

$$n_{pf}^o = n_{(L_F)} \exp\left(\frac{RL_F}{G\tau}\right) \tag{7}$$

The nucleation rate was calculated from

$$B^o = n_{pf}^o G \tag{8}$$

Values obtained for B^o are given in Table 3. From the calculated value of n_{pf}^o and the known values of τ, G, and R, the portion of Equation (1) describing the CSD

less than L_F was drawn on Figures 5 to 9. This calculated curve is in excellent agreement with the actual experimental CSD for this size range. It should be emphasized that the parameters for this portion of the curve were determined from known flow rates, calculated settling velocities, and from the analysis of the CSD of the larger sizes. Only in one case (Figure 7) was an alternate procedure used to determine the slope and intercept of the small crystal size range. There were too few experimental points to determine the slope precisely; therefore, the nucleation rate was determined by curve fitting both portions of the CSD curve. For this purpose, Equation (1) was transformed to

$$Y = Y_o + SX \tag{9}$$

where

$$Y = \ln n \tag{10}$$

$$Y_o = \ln n_{pf}^o \tag{11}$$

$$S = -\frac{R}{G\tau} \tag{12}$$

and

$$X = L \qquad L < L_F$$
$$X = \left(\frac{R-1}{R} L_F + \frac{L}{R}\right) \qquad L > L_F \tag{13}$$

n_{pf}^o and G were determined using the method of least squares.

Nucleation Rate Assuming Laminar Flow

The model described below is proposed for use when flow in the fines trap deviates from plug flow. For the liquor in the trap, the parabolic velocity distribution is given by

$$\frac{u}{u_{\max}} = 1 - \left[\frac{2r}{D}\right]^2 \tag{14}$$

Moreover

$$u_{\max} = 2\bar{u} \tag{15}$$

Clearly, the above assumed flow profiles are symmetrical around the axis, and the flow velocity u is related to its radial position by

$$r = \frac{D}{2}\left(1 - \frac{u}{u_{\max}}\right)^{0.5} \tag{16}$$

At $r = D/2$, $u = 0$ and at $r = 0$, $u = u_{\max}$. The volumetric flow rate can be expressed as a function of r by

$$dQ_R = 2\pi r u dr \tag{17}$$

and the part of the suspension that flows through the trap with a velocity greater than $u(r)$ is equal to

$$Q_R(u) = \int_o^r 2\pi r u dr \tag{18}$$

Solving and incorporating Equation (16), we get

$$Q_R(u) = \frac{\pi D^2 u_{\max}}{8}\left[1 - \left(\frac{u}{u_{\max}}\right)^2\right] \tag{19}$$

or, using Equation (15), we get

$$Q_R(u) = \pi \frac{D^2}{4}\bar{u}\left[1 - \left(\frac{u}{2u}\right)^2\right] \tag{19a}$$

Now, let crystals of size L be the largest crystals that will be removed in a stream with velocity u. This velocity u would then necessarily be the settling velocity of crystal of size L. By approximating the relationship between settling velocity and size by

$$u = k_L L^m \tag{20}$$

an expression describing removal velocity of particles of size L can be obtained by combining Equations (19) and (20) as follows:

$$Q_R(L) = \frac{\pi D^2}{4}\bar{u}\left[1 - \left(\frac{k_L}{2\bar{u}}\right)^2 L^{2m}\right] \tag{21}$$

Including Equation (21) in the population balance for an MSMPR crystallizer with fines dissolving gives

$$VG\frac{dn}{dL} = -nQ - nQ_R(L) \qquad L < L_{\max}$$
$$VG\frac{dn}{dL} = -nQ \qquad L > L_{\max} \tag{22}$$

with the following solution:

$$n = n_{1f}^o \exp\left[-\frac{RL}{G\tau}\zeta(L)\right] \qquad L < L_{\max}$$
$$n = C_2 \exp\left[-\frac{L}{G\tau}\right] \qquad L > L_{\max} \tag{23}$$

The function $\zeta(L)$ in Equation (23) has the form

$$\zeta(L) = 1 - \frac{(k_L A)^2}{4(2m+1)R(R-1)Q} L^{2m} \tag{24}$$

In the analysis of experimental results for the purpose of calculating n_{1f}^o, A and R were taken from experimental conditions, and C_2 and G were obtained from the straight line representing the middle portion of the experimental distribution. k_L and m were determined from the settling data given in Figure 10. For the purpose of this analysis, two equations were used to describe the settling velocity of the crystals:

$$u = 4.68 \times 10^{-4} L^{1.6} \quad 70\ \mu\text{m} < L < 250\ \mu\text{m} \tag{25}$$

and

$$u = 1.29 \times 10^{-4} L^{1.9} \quad 30\ \mu\text{m} < L < 130\ \mu\text{m} \tag{26}$$

It was found that the assumption of laminar flow gives, in effect, a better correspondence with the data only over the narrow range from $L_{\max}$ to L_F, while for small crystal sizes it predicts higher numbers than were observed. The results of these computations are also given in Table 3 and are shown as dotted lines on the size distribution plots shown in Figures 5 to 9.

DISCUSSION OF RESULTS

The experimental results presented in this paper confirm the CSD model developed by Randolph and Larson for continuous crystallizers with fines removal and destruction systems. These results also show that the model can be modified to account for nonideal fines separation and removal. The accuracy of measurement was adequate to establish the effect of fines dissolving and showed that theoretical predictions could be realized by experiment. The cut size L_F predicted from independent settling velocity data was confirmed by experiment, as was the slope of the small crystal size distribution determined a priori from the recycle ratio R. Repeated sampling during runs gave good consistency of results. Samples taken from the body of the crystallizer gave CSD in good agreement with samples taken from the fines removal system for the small crystal size range. Only when sampling from the fines removal system was done very slowly was in-

consistency found. This inconsistency can be attributed to dissolution of fines during sampling, because the sampling reservoir was normally 6°C warmer than the crystallizer body. In these instances, the populations of all sizes were reduced proportionally.

Comparing the experimental distributions with those produced by assuming plug flow or laminar flow in the fines trap did not conclusively show which flow model was best suited. For the smallest size range, the plug flow model gave the best prediction. For the size range in the region near L_{max}, the laminar flow model gave the best prediction, but for the smaller sizes it predicted greater populations than observed, although the slope of the distribution curve was the same as the experimental data line. Clearly, the fines trap used was of insufficient length for the full parabolic flow profile to be established, and it must be concluded that the velocity profile deviated only slightly from plug flow.

It is also possible that classification in the crystallizer occurred, which resulted a high concentration near the point of discharge, of the larger crystals from the middle portion of the size range. This concentration would result in a greater fraction of these crystals being removed than is predicted by the crystallizer retention time, τ. The resulting bias would result in a calculated growth rate smaller than the actual rate. On the other hand, classification such that the population of large crystals was low in the region of discharge would give calculated growth rates larger than actual. In some instances this phenomenon would give a curved semilog CSD plot, prompting a false conclusion that growth was size dependent. It was clear, however, that in these experiments the above effects were imperceptible in the size range from L_{max} to L_C, and it was from this size range that growth rate was determined. It should also be noted that even if some error were introduced because of these effects, it would apply equally to both fines dissolving runs and MSMPR runs. Thus, the conclusions drawn in regard to the fines dissolving model remain unchanged.

The nucleataion kinetics correlation in Figure 12 shows that the experimental results for fines dissolving runs give higher nucleation kinetic rates than did MSMPR runs. The combined correlation of the results of both kinds of experiments gives a kinetic relationship

$$B^o = 1.23\, M_T^{0.5} G^{2.65} \qquad (27)$$

The MSMPR data taken alone give an order of nucleation of 2.06 rather than 2.65. As is shown in Tables 2 and 3, the growth rates and therefore the supersaturation in the fines dissolving runs were substantially higher. This suggests that the power law kinetics may not be suitable for a wide range of supersaturations and that for design purposes the range acceptable for application of experimental data is limited. This lack of agreement apparently lies in our lack of understanding of the secondary nucleation phenomenon. Net secondary nucleation rate is closely related to nuclei survival which in turn is very sensitive to supersaturation level.

The recirculation of undissolved crystals could also cause an appparent higher nucleation rate under conditions of fines destruction. The data presented here, however, are only for those runs where total destruction of fines in the fines removal was achieved. The matter of partial dissolution of the fines in the fines removal system will be considered in a separate paper.

ACKNOWLEDGMENT

The authors wish to acknowledge the support of Polytechnical University of Warsaw, The Iowa State Engineering Research Institute, and the National Science Foundation through grant number 7303764.

NOTATION

A = value of an active flow area in a trap
B^o = nucleation rate, No/ls
$B_{1f}{}^o$ = nucleation rate calculated from laminar flow model
$B_{pf}{}^o$ = nucleation rate calculated from plug flow model
C_1 = constant in Equation (3) defined by the expression /4/
C_2 = constant in Equation (23)
D = diameter of a trap
d_s = spherical particle diameter
G = linear growth rate of crystals
i = exponent on G in power law nucleation kinetics expression
j = exponent on M in power law nucleation kinetics expression
k_L = proportionality rate constant in expression (20)
k_n = proportionality rate constant in nucleation kinetics expression
L = crystal size, function described by (24)
$\overline{L}$ = average crystal size
L_c = limit size of classified product removal
L_F = limit size fines removal
L_{max} = biggest size of fines removal in the laminar flow model
m = exponent on L in expression (20)
M_T = density of suspension, g/l
n = crystal population density, No/1 μm
n^o = population density of nuclei
$n_{1f}{}^o$ = population density of nuclei calculated from laminar flow model
$n_{pf}{}^o$ = population density of nuclei from plug flow model
Q = mixed discharge flow rate, feed flow rate
Q_R = volumetric velocity of fines removal
r = radius
R = ratio of fines removal to mixed discharge rates, $L < L_F$
R_e = Reynold's number for flow through a trap
S = constant defined by expression (12), negative slope
$\overline{u}$ = mean linear velocity of a suspension flow in a trap
u = linear velocity of flow
$\overline{u_s}$ = average sedimentation velocity of potassium nitrate crystals with size $\overline{L}$
u_{max} = maximum linear velocity of fluid for laminar flow
V = total volume of suspension
X = abscissa in Equation (9)
Y = ordinate in Equation (9)
Y_o = constant in Equation (9)
z = ratio of oversize product discharge rate to mixed discharge rate, $L > L_c$
τ = mean drawdown time of crystallizer

LITERATURE CITED

Helt, J. E., and M. A. Larson, "Effect of Temperature on the Crystallization of Potassium Nitrate by Direct Measurement of Supersaturation," *AIChE J.* (in press).

Randolph, A. D., "The Mixed Suspension, Mixed Product Removal Crystallizer as a Concept in Crystallizer Design," *ibid.*, 11, 429 (1965).

Randolph, A. D., and M. A. Larson, *Theory of Particulate Processes*, pp. 135-138, Academic Press, New York (1971).

Saeman, W. C., "Crystal-Size Distributions in Mixed Suspensions," *AIChE J.*, 2, 107 (1956).

Manuscript received January 31, 1977; revision received April 25, and accepted April 27, 1977.